

# Invariant representation of mean inertia provides a theoretical basis for the log law in turbulent boundary layers

**J. Klewicki<sup>1,2</sup>**

<sup>1</sup>Department of Mechanical Engineering  
University of New Hampshire

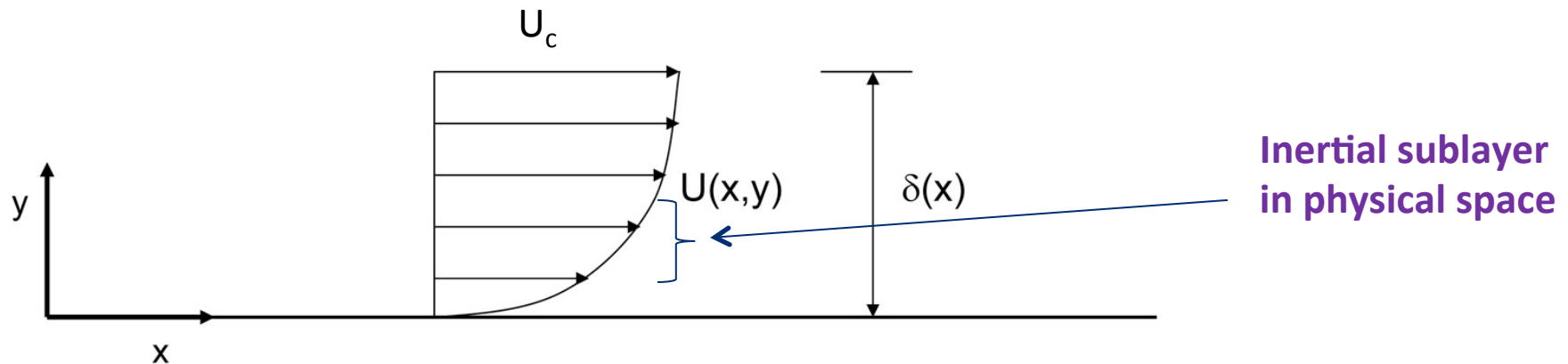
<sup>2</sup>Department of Mechanical Engineering  
University of Melbourne

Collaborators: Caleb Morrill-Winter, Jimmy Philip, Martin Oberlack, Paul Fife, Ivan Marusic  
and others

This research was supported by the NSF and ARC

# Inertial Logarithmic Region

Consider a turbulent wall-flow,



$\delta$  = channel half-height, boundary layer thickness

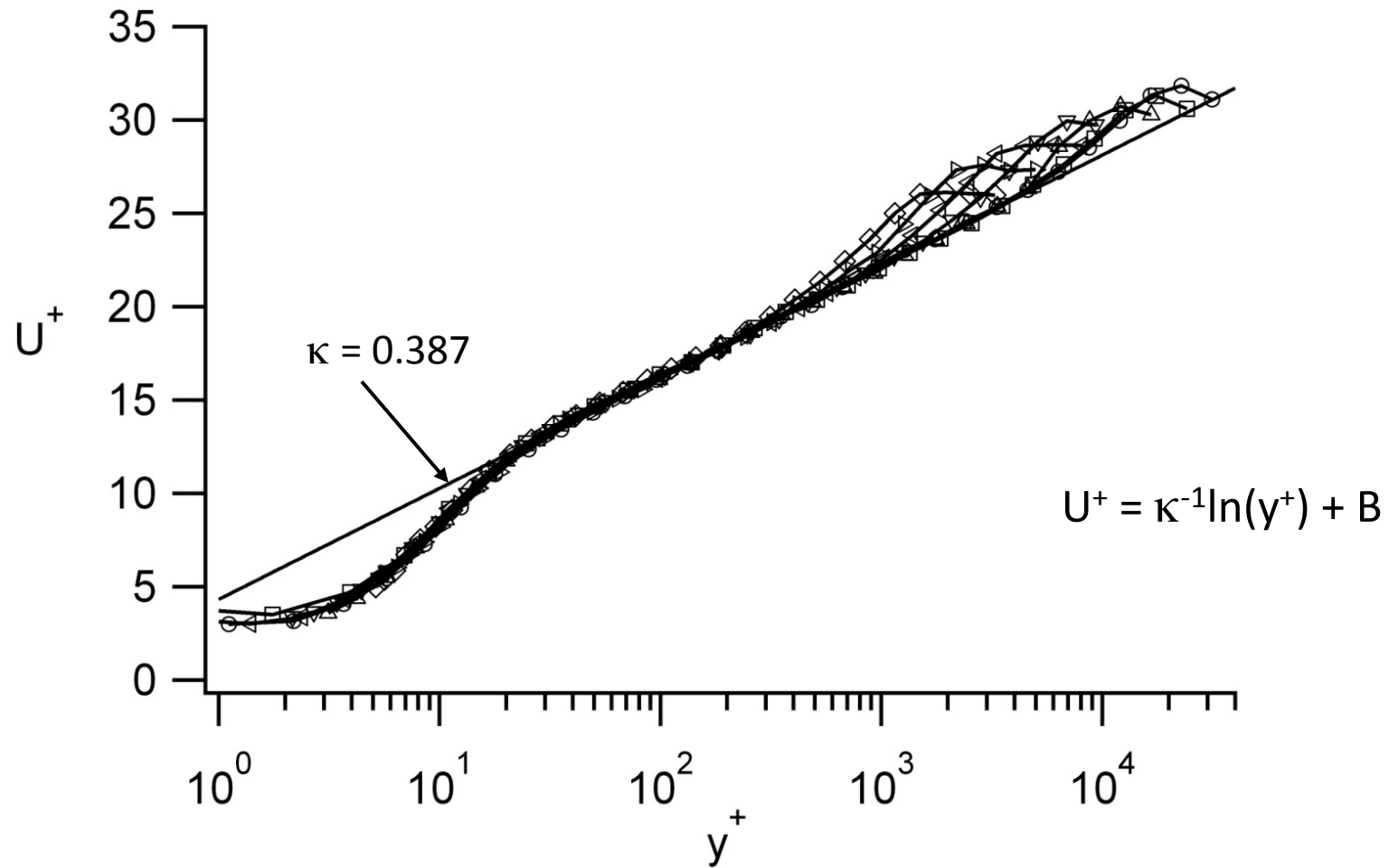
$u_\tau$  = friction velocity =  $(\tau_w/\rho)^{1/2}$  = characteristic velocity scale

$y^+$  =  $y u_\tau / \nu$  = inner-normalized distance from the wall

$\eta$  =  $y/\delta$  = outer-normalized distance from the wall

$\delta^+$  =  $\delta u_\tau / \nu$  = Reynolds number (ratio of outer to inner length)

# Logarithmic Mean Velocity Profile



Vincenti et al. (2013), FPF

# Logarithmic Mean Velocity Profile Slope

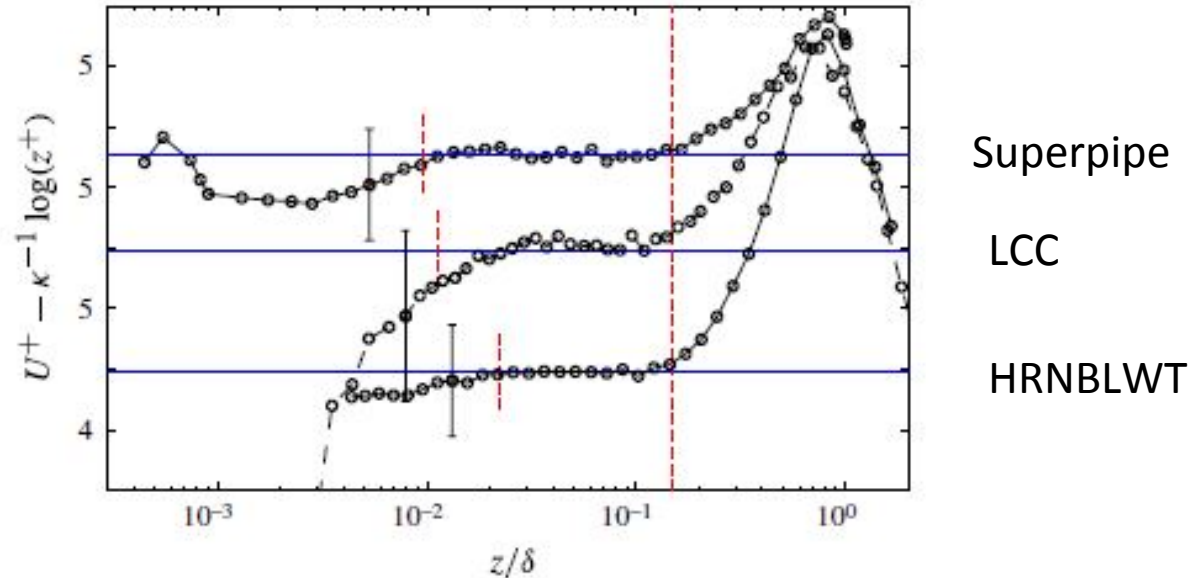


FIGURE 3. Mean velocity profiles with log law function, where  $\kappa = 0.39$ , subtracted for the Superpipe, LCC and Melbourne datasets (shown in order from top to bottom). The dashed vertical lines indicate the region  $3Re_\tau^{1/2} < z^+ < 0.15Re_\tau$ , and the horizontal lines indicate the best fit for this range highlighting the log region plateau. Error bars of  $U^+$  are shown at the indicated locations.

Marusic et al. (2013)

# K Estimates Over Time

$\approx 0.38$	von Karman (1930)
0.41	Coles (1968)
0.4	Yaglom (1974)
$0.38 \pm 0.04$	Francey & Garrett (1981)
$0.40 \pm 0.011$	Hogstrom (1985)
$0.387 \pm 0.01$	Frenzen & Vogel (1985)
$0.436 \pm 0.002$	Zagarola & Smits (1998)
0.38	Osterlund (2000)
$\approx 0.39$	Perry, Hafez & Chong (2001) ["corrected" Z & S data]
$0.421 \pm 0.002$	McKeon (2004)
0.387	Andreas et al. (2006)
0.384	Nagib, Chauhan, Monkewitz (2007)
$0.389 \pm 0.004$	Klewicki, Fife & Wei (2009), [dW/dy at $\delta^+ = 2004$ ] (Hoyas & Jimenez data)
0.39	Marusic et al. (2013) [four high Reynolds number facilities]
0.383, [0.384]	Pirozzoli (2014), [dW/dy at $\delta^+ = 4080$ ]
$0.4 \pm 0.02$	Bailey et al. (2014)
0.381966...	Klewicki et al. (2014), [ $\delta^+ \rightarrow \infty$ extension]
0.384, [0.383]	Lee and Moser (2015) [dW/dy at $\delta^+ = 5200$ ]
0.382	Furuichi et al. (2015)

# Rationalizing the Log Law

i) Prandtl:  $dU/dy \propto u_\tau/y$

Leads to

$$dU^+/dy^+ = (\kappa y^+)^{-1}$$

*(distance from the wall scaling hypothesis)*

ii) Millikan:  $U^+ = f(y^+)$ ,  $U^+ - U_\infty^+ = F(\eta)$

Leads to

$$y^+ dU^+/dy^+ = \eta dU^+/d\eta = \kappa^{-1}$$

*(inner/outer/overlap hypothesis)*

**Is there a better justification?**

# Scaling

Scaling comes from the symmetries admitted by the relevant governing equation, i.e., when the equation is recast according to the transformations indicated by the admitted symmetries, it becomes *invariant* to changes in the underlying parameters.

Conversely, if the governing equation does not admit an *invariant form*, there is little (no) reason to expect the variable of interest can be scaled.

**Thus, it is rational to expect that the universal logarithmic constitutes a similarity solution stemming from an invariant representation of the governing equation**

**(e.g., like what is done for laminar similarity solutions)**

# Four Layer Structure

## Channel & Boundary Layer

### (multiple leading order balances)

## Mean Momentum Balances

### Pipe & Channel

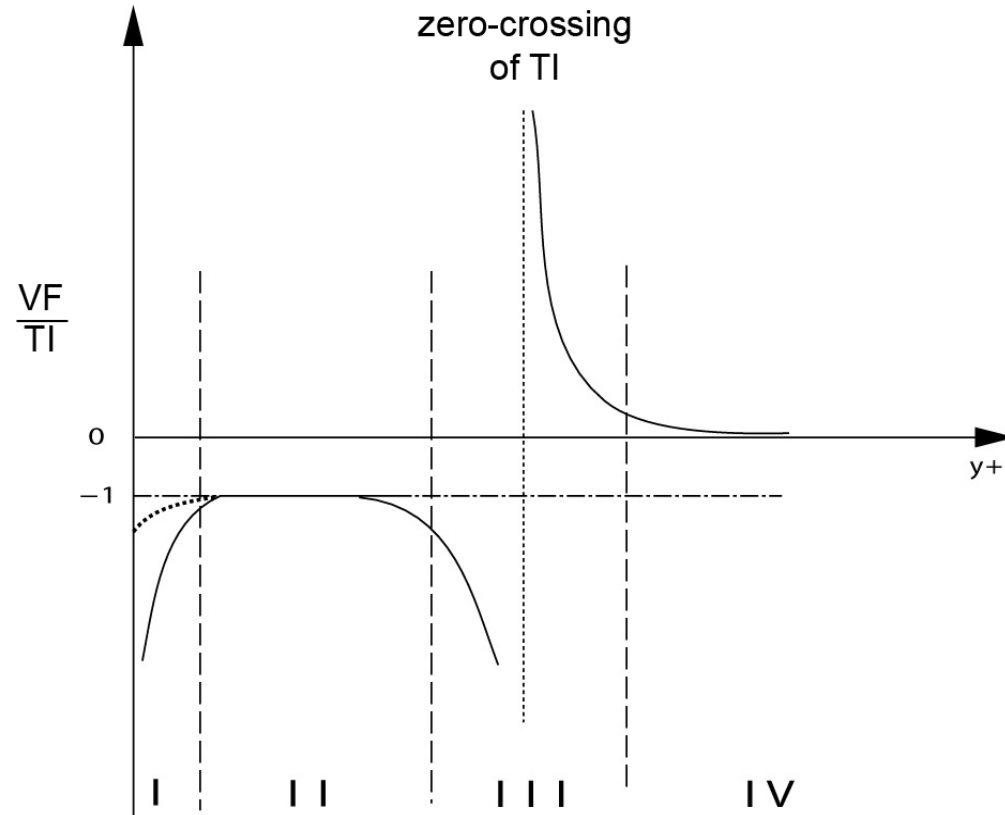
$$\frac{d^2U^+}{dy^{+2}} + \frac{dT^+}{dy^+} + \epsilon^2 = 0$$

$$\text{VF} \quad \text{TI} \quad \text{PG} \quad (\epsilon^2 = 1/\delta^+)$$

### Boundary Layer

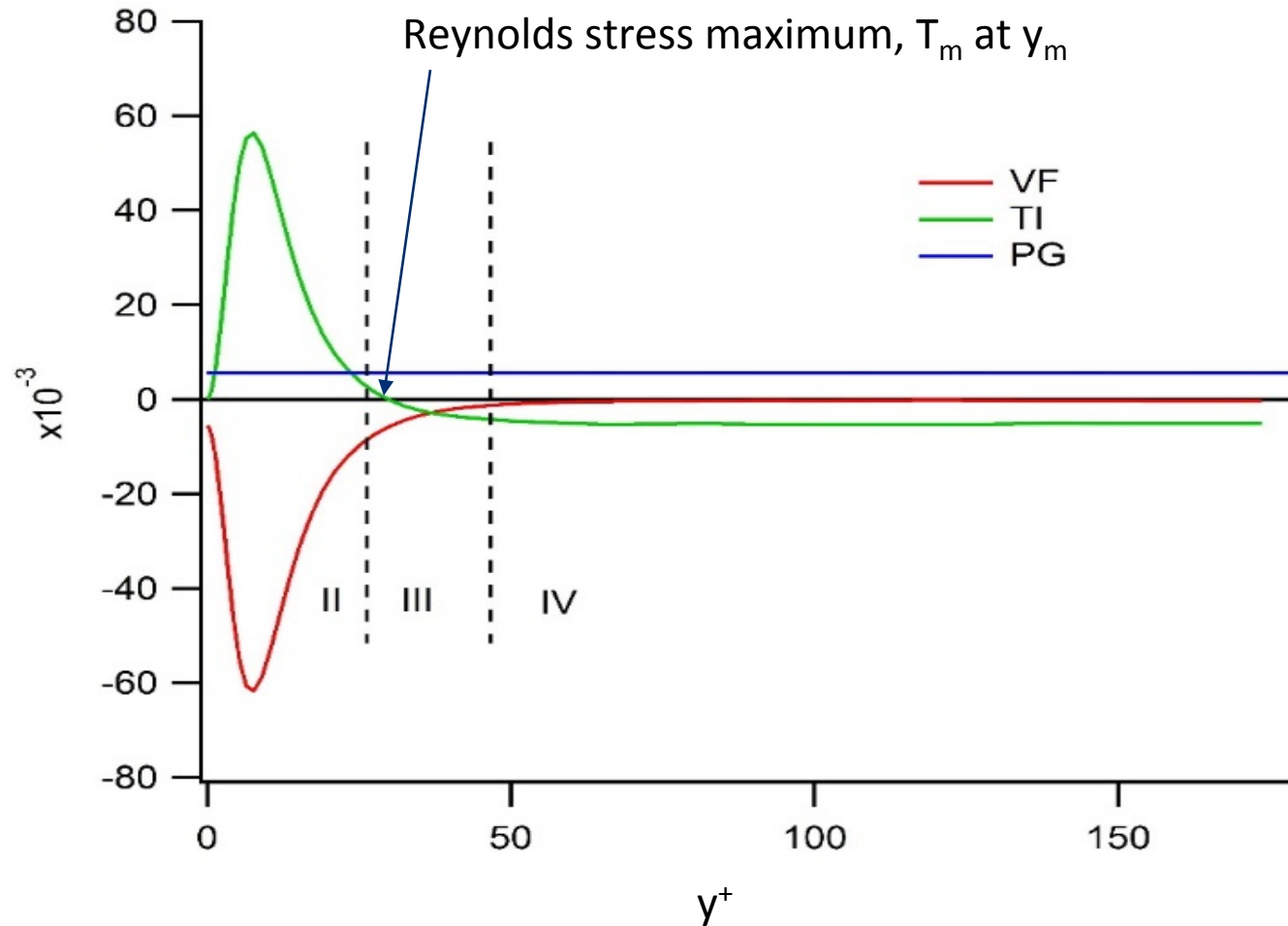
$$U^+ \frac{\partial U^+}{\partial x^+} + V^+ \frac{\partial U^+}{\partial y^+} = \frac{\partial^2 U^+}{\partial y^{+2}} - \frac{\partial \overline{uv}^+}{\partial y^+}$$

$$\text{MI} \quad \text{VF} \quad \text{TI}$$



Wei et al. JFM (2005)

# Layer III Structure



$\delta^+ = 180$  channel DNS  
Hoyas & Jimenez PoF (2006)

# Layer III Rescaling

In layer III all the terms are of the same order of magnitude (except right at  $y_m$ ), and thus the goal is to find a scaling that renders all of the terms  $O(1)$ . To this end, let,

$$dy^+ = \alpha d\hat{y}, \text{ and } dT^+ = \gamma' d\hat{T},$$

and require that,

$$\frac{d^2U^+}{d\hat{y}^2} \text{ and } \frac{d\hat{T}}{d\hat{y}} \text{ be } O(1)$$

This yields,

$$d\hat{y} = \epsilon dy^+, \text{ and } dT^+ = \epsilon d\hat{T} \quad (\epsilon = 1/\sqrt{\delta^+})$$

# Layer III Rescaling (continued)

With this transformation, the mean momentum equation becomes,

$$\frac{d^2 U^+}{d\hat{y}^2} + \frac{d\hat{T}}{d\hat{y}} + 1 = 0$$

with

$$(\epsilon^2 = 1/\delta^+)$$

$$y^+ = y_m^+ + \frac{1}{\epsilon}\hat{y}, \quad T^+ = T_m^+ + \epsilon\hat{T}$$

(i.e., the “hat” variables are centered around the peak in  $T^+$ )

# Invariance Across a Hierarchy of Scaling Layers

Fife et al. DCDS (2009)

Plugging

$$T_{\beta}^+ = T^+(y^+) + \frac{y^+}{\delta^+} - \beta y^+ \quad \text{“Adjusted Reynolds stress”}$$

into

$$0 = \frac{1}{\delta^+} + \frac{d^2 U^+}{dy^{+2}} + \frac{dT^+}{dy^+}$$

yields

$$0 = \beta + \frac{d^2 U^+}{dy^{+2}} + \frac{dT_{\beta}^+}{dy^+}$$

$$\begin{aligned} & \underbrace{T^+}_{T^+ + \varepsilon^2} \\ & \frac{dT^+}{dy^+} + \frac{1}{\delta^+} - \beta \end{aligned}$$

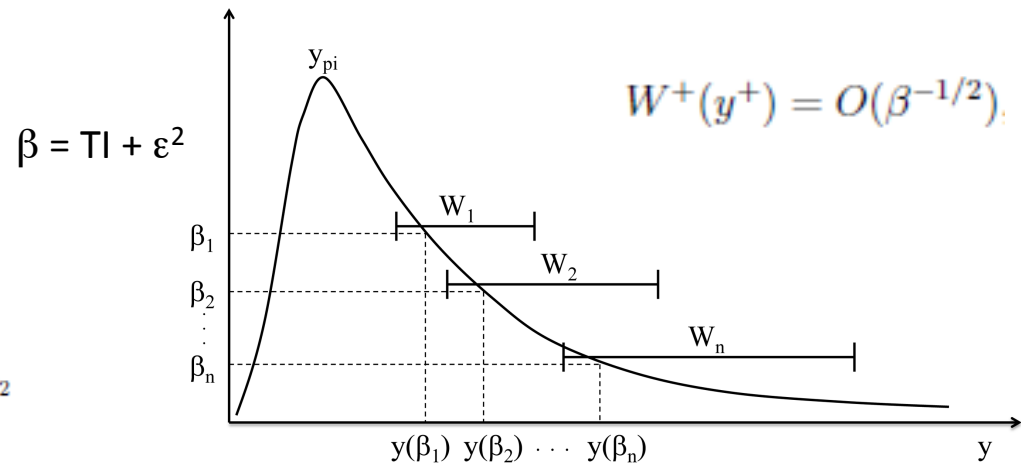
Then using

$$y^+ = y_{\beta}^+ + \beta^{-1/2} \hat{y}, \quad T^+ = T_m^+(y_{\beta}^+) + \beta^{1/2} \hat{T}(\hat{y}), \quad U^+ = U^+(y_{\beta}^+) + m(y_{\beta}^+)(y^+ - y_{\beta}^+) + \lambda \hat{U}(\hat{y})$$

yields the invariant form

$$\frac{d^2 U^+}{dy^{+2}} + \frac{d\hat{T}}{d\hat{y}} + 1 = 0.$$

$$A = -\frac{d^2 \hat{T}}{d\hat{y}^2} = -\frac{d^2 T^+}{dy^{+2}} \left( \frac{dT^+}{dy^+} + \frac{1}{\delta^+} \right)^{-3/2} = -\frac{d^2 T^+}{dy^{+2}} \beta^{-3/2}$$



# Condition for Self-Similarity

On each layer the condition for dynamic self-similarity

$$A(\beta) = -\frac{d^2 \hat{T}_\beta}{d\hat{y}^2} (\hat{y} = 0)$$

“hat” variables are normalized by  $W$  and  $u_\tau$ .

is asymptotically approached. i.e., the normalized curvature of the Reynolds stress profile becomes invariant from one layer to the next

Physically, the normalized flux of turbulent inertial force attains **constancy** on the portion of the scaling layer hierarchy where the leading order mean dynamics are wholly inertial – i.e., in layer IV

# Coordinate Stretching

It is also analytically known that,

$$dW/dy = A/2 = \phi^{-1} \quad \begin{array}{l} \text{Origin of} \\ \text{“distance from the wall”} \\ \text{scaling} \end{array}$$

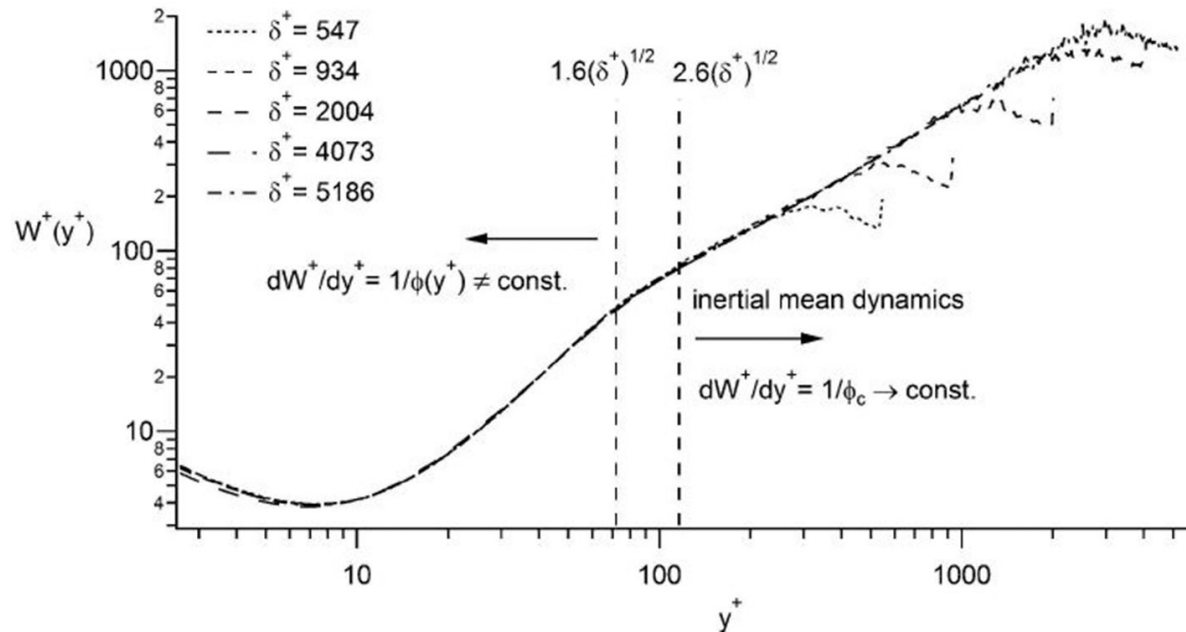
where  $\phi$  (Fife similarity parameter) is the coordinate stretching function that yields the invariant form:

$$\frac{d^2 U^+}{d\hat{y}^2} + \frac{d\hat{T}}{d\hat{y}} + 1 = 0.$$

According to this theory, on the **inertial domain** of interest,  $\phi \rightarrow \phi_c$ , and von Karman's constant is given by two equivalent relations:

- $\kappa = \phi_c^{-2}$ , is a function of the constant coordinate stretching underlying asymptotic self-similarity, or
- $\kappa = A^2/4$ , is associated with the asymptotically constant flux of turbulent inertial force

# Layer Width Distribution



Physically,  $W$  is the size of the  $-\langle uv \rangle^+$  motions

FIG. 1. Distribution of  $W^+(y^+)$  for channel flows. Profiles at  $\delta^+ = 547, 934$  and  $2004$  are from the study of Hoyas and Jiménez.<sup>22</sup> The profile at  $\delta^+ = 4073$  is from Pirozoli,<sup>23</sup> and the profile at  $\delta^+ = 5186$  is from Lee and Moser.<sup>24</sup> Vertical lines denoting the beginning and end of layer III are shown for  $\delta^+ = 2004$ .

Linear  $W(y^+)$  in layer IV provides equation based reason for *distance-from-the-wall* scaling

# Channel Similarity Solution

Recall the transformation that yields the invariant form of the mean momentum equation

$$\frac{1}{\phi} = -\frac{1}{2} \frac{d^2 \hat{T}}{d\hat{y}^2} = -\frac{1}{2} \frac{d^2 T^+}{dy^{+2}} \left( \frac{dT^+}{dy^+} + \frac{1}{\delta^+} \right)^{-3/2} = -\frac{1}{2} \frac{d^2 T^+}{dy^{+2}} \left( -\frac{d^2 U^+}{dy^{+2}} \right)^{-3/2} \quad (1)$$

The exact channel flow mean vorticity equation is,

$$0 = -\frac{d^2 \Omega_z^+}{dy^{+2}} + \frac{d^2 T^+}{dy^{+2}}, \quad (2)$$

where  $\Omega_z = -dU/dy$ . Setting  $\phi = \text{const.}$  (not necessarily  $\phi_c$ ) and combining with the third equality in (1) yields

$$\frac{2}{\phi} = \frac{d^3 U^+}{dy^{+3}} \left( -\frac{d^2 U^+}{dy^{+2}} \right)^{-3/2}. \quad (3)$$

# Analytical Integration

(Klewicki & Oberlack 2015)

Let  $f = -d^2U^+/dy^{+2}$ , and then (3) becomes

$$\frac{2}{\phi} f^{3/2} = -\frac{df}{dy^+}. \quad (4)$$

Separating variables and integrating yields

$$f^{-1/2} = \frac{1}{\phi}(y^+ - y_0^+), \quad (5)$$

and squaring and inverting this result gives

$$f \equiv -\frac{d^2U^+}{dy^{+2}} = \phi^2(y^+ - y_0^+)^{-2}. \quad (6)$$

Two more integrations yield the final result

$$U^+ = \phi^2 \ln(y^+ - y_0^+) + By^+ + C. \quad (7)$$

The Reynolds stress,  $T^+$ , is then found from the exact relation,

$$\frac{dU^+}{dy^+} = 1 - T^+ - \frac{y^+}{\delta^+}, \quad (8)$$

**Note that the BC on  $dU^+/dy^+$  requires that  $B \rightarrow 0$  as  $y^+ \rightarrow \infty$  (i.e., as  $\delta^+ \rightarrow \infty$ ).**

# Finite Reynolds Number Behaviours (traditional representation)

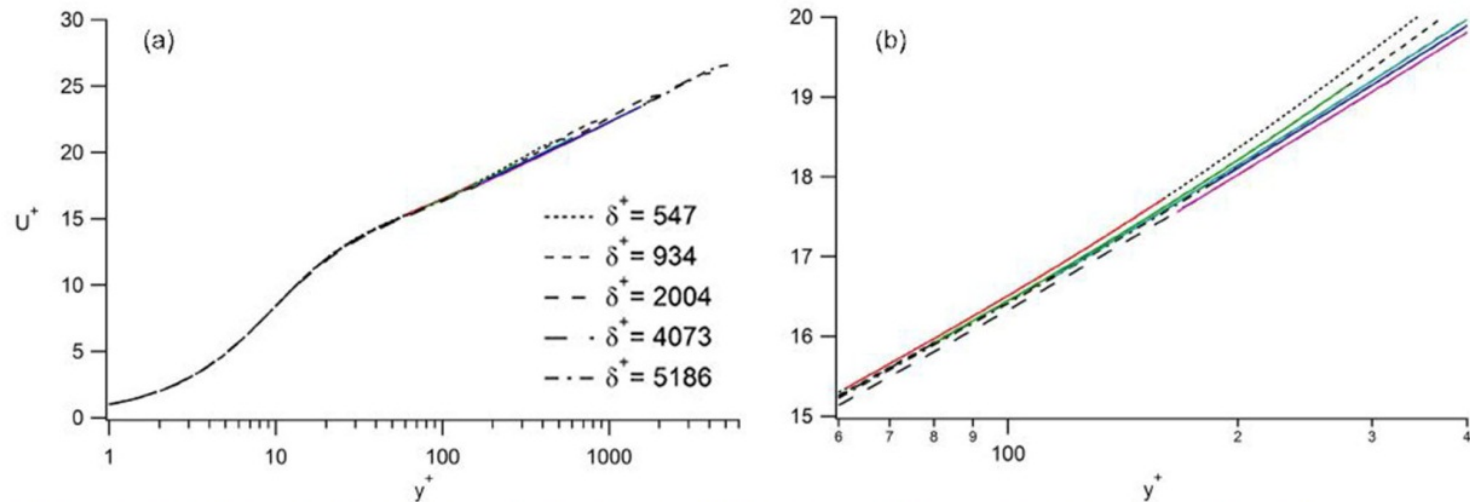


FIG. 2. Profiles of  $U^+$  versus  $y^+$  for channel flows, and their comparison with the best fits of (16) for  $y_0^+ = 0$  over the domain  $2.6\sqrt{\delta^+} \lesssim y^+ \lesssim 0.3\delta^+$ ; (a) full profiles, (b) closeup of the inertial domain. Profiles at  $\delta^+ = 547, 934$  and  $2004$  are from the study of Hoyas and Jiménez.<sup>22</sup> The profile at  $\delta^+ = 4073$  is from Pirozoli,<sup>23</sup> and the profile at  $\delta^+ = 5186$  is from Lee and Moser.<sup>24</sup> Line styles of the DNS data are the same as in Fig. 1. The curve fits (color online) are the solid lines that overlay the data.

# Finite Reynolds Number Behaviours (similarity solution representation)

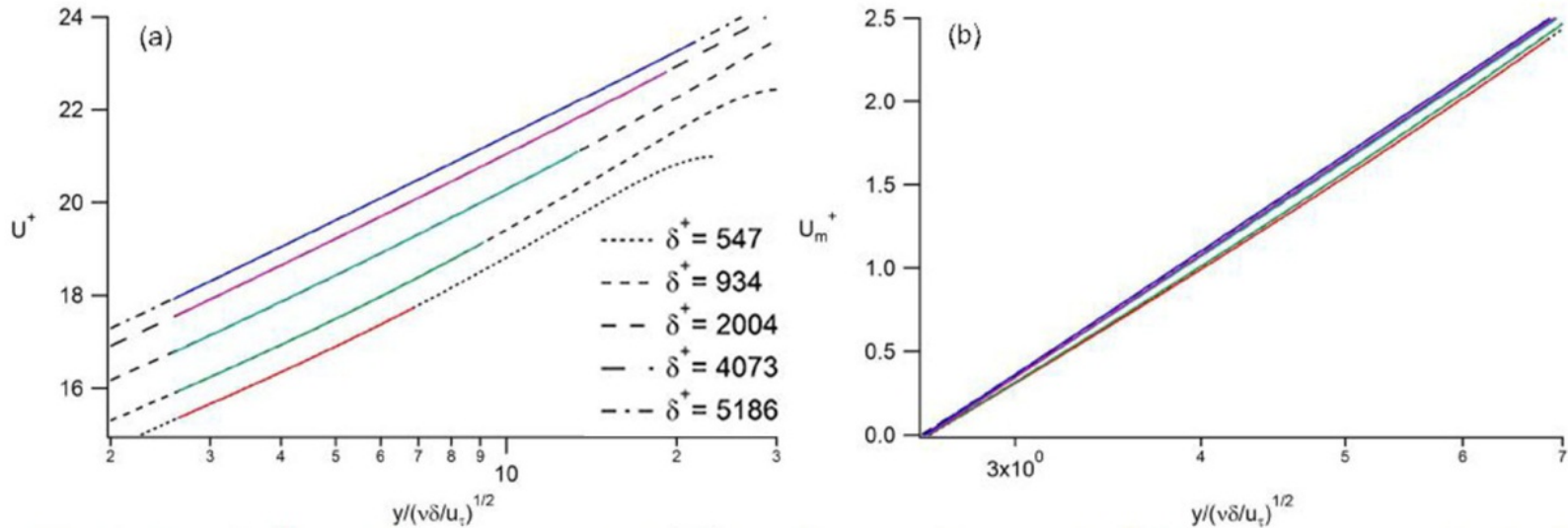


FIG. 3. (a) Profiles of  $U^+$  versus  $y^+/\sqrt{\delta^+}$  for channel flows, and their comparison with the best fits of (16) for  $y_0^+ = 0$  over the domain  $1 \lesssim y^+/\sqrt{\delta^+} \lesssim 0.3\sqrt{\delta^+}$ ; (b) Profiles of  $U_m^+ = U^+ - U_s^+$  on the lower part of the inertial domain. Profiles at  $\delta^+ = 547$ , 934 and 2004 are from the study of Hoyas and Jiménez.<sup>22</sup> The profile at  $\delta^+ = 4073$  is from Pirozoli,<sup>23</sup> and the profile at  $\delta^+ = 5186$  is from Lee and Moser.<sup>24</sup> Line styles of the DNS data are the same as in Fig. 1. The curve fits (color online) are the solid lines that overlay the data.

# Log-Linear Law Coefficients

$$U^+ = \phi^2 \ln(y^+ - y_0^+) + By^+ + C$$

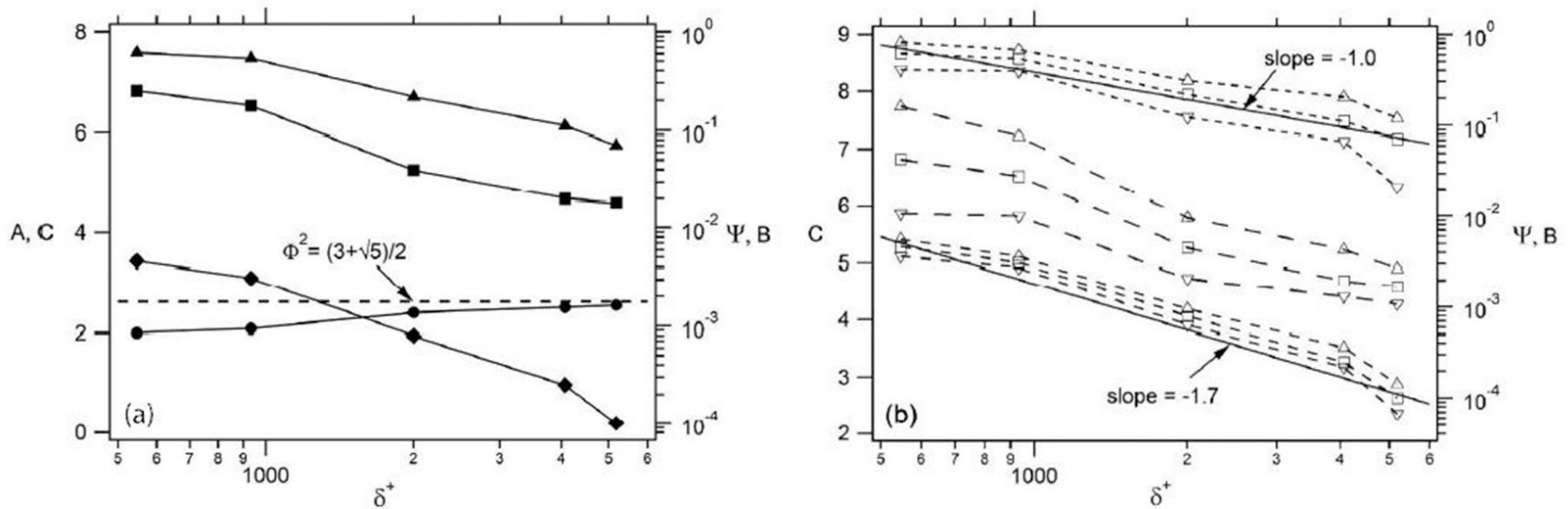


FIG. 4. (a) Curve-fit coefficients in (16) for  $y_0^+ = 0$  versus  $\delta^+$ .  $\bullet$ ,  $A \rightarrow \phi_c^2$ ;  $\blacklozenge$ ,  $B$ ;  $\blacksquare$ ,  $C$ ;  $\blacktriangle$ ,  $\Psi = \Phi^2 - A$ . Dashed line is the square of the golden ratio,  $\Phi = (1 + \sqrt{5})/2$ . (b) Curve-fit coefficients for different  $y_0^+$ ;  $\triangle$ ,  $y_0^+ = 5$ ;  $\square$ ,  $y_0^+ = 0$ ;  $\nabla$ ,  $y_0^+ = -5$ ;  $- - -$ ,  $B$ ;  $- \quad -$ ,  $C$ ;  $- \cdot - \cdot -$ ,  $\Psi$ .

# ZPG Boundary Layer Analysis

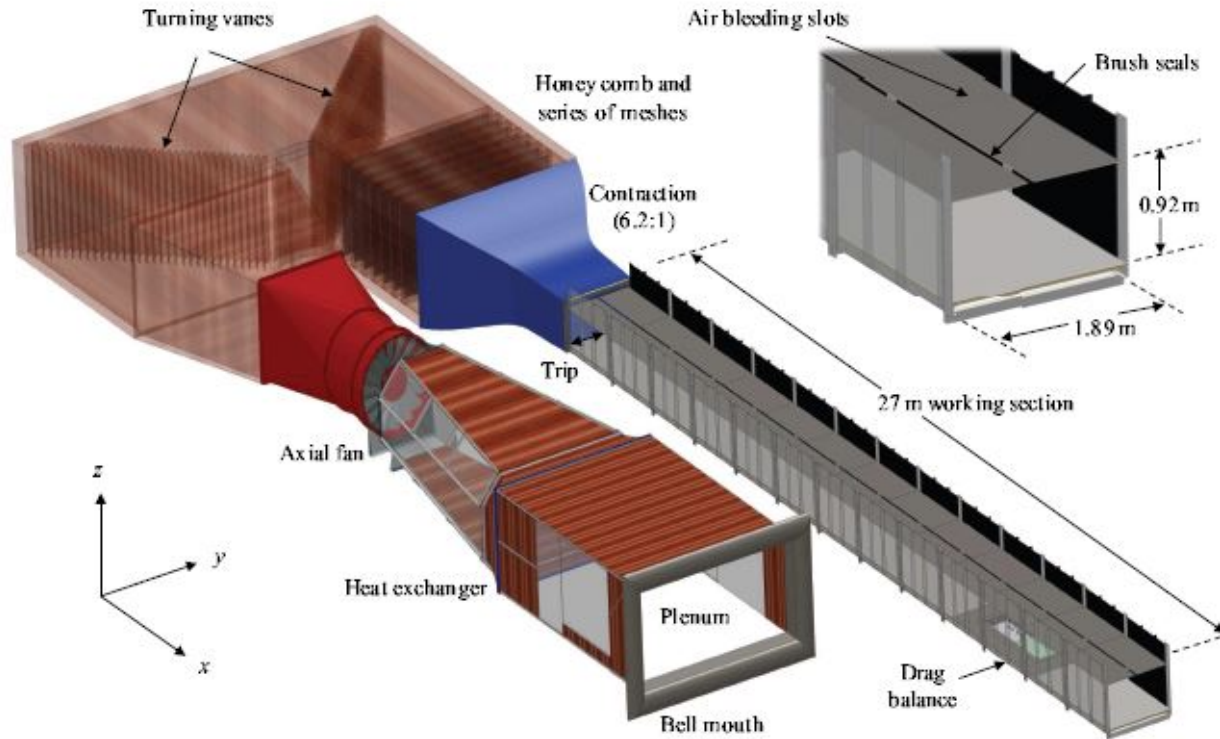
(Morrill-Winter et al. JFM 2017, in press)

Can we recast the mean momentum equation for the boundary layer

$$\underbrace{\frac{\partial^2 U^+}{\partial y^{+2}}}_{\text{VF}} + \underbrace{\frac{\partial T^+}{\partial y^+}}_{\text{TI}} + \underbrace{\overline{A^+}}_{\text{MI}} = 0$$

in a form that represents the mean inertia (MI) term  $A^+ = U^+ dU^+/dx^+ + V^+ dU^+/dy^+$  as a only function of  $\delta^+$ ?

# High Reynolds Number Boundary Layer Wind Tunnel (Melbourne)



# Flow Physics Facility

(New Hampshire)

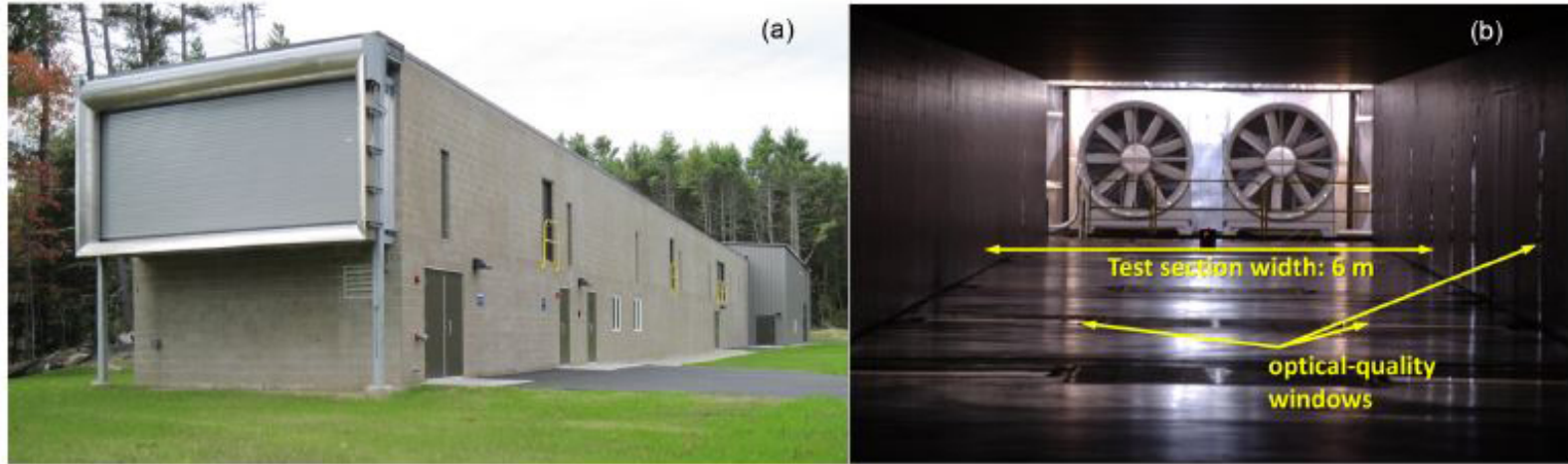
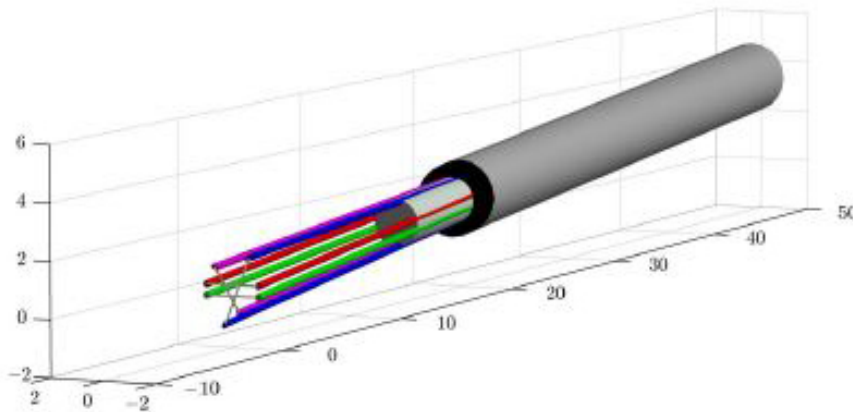


Figure 10: (a) FPF wind tunnel, flow enters the test section through the inlet at the front and discharges into the plenum at the rear, (b) View down the test section into the discharge plenum.

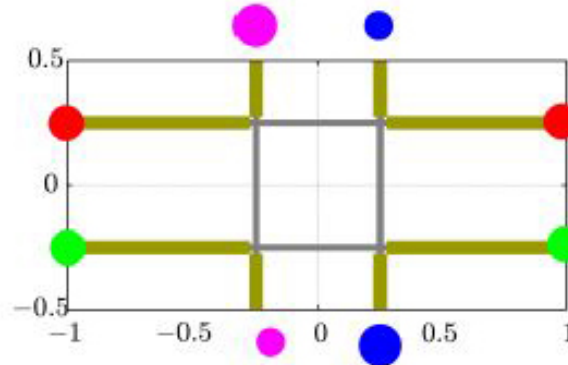
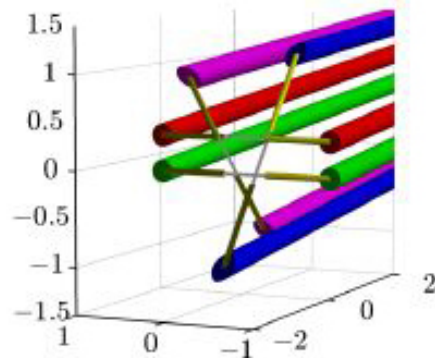
# Mini-Spanwise Vorticity Probe

(Morrill-Winter et al. Eif 2015)

mini-Foss style probe



\*units are in mm



# HRNBLWT and FPF Data Sets

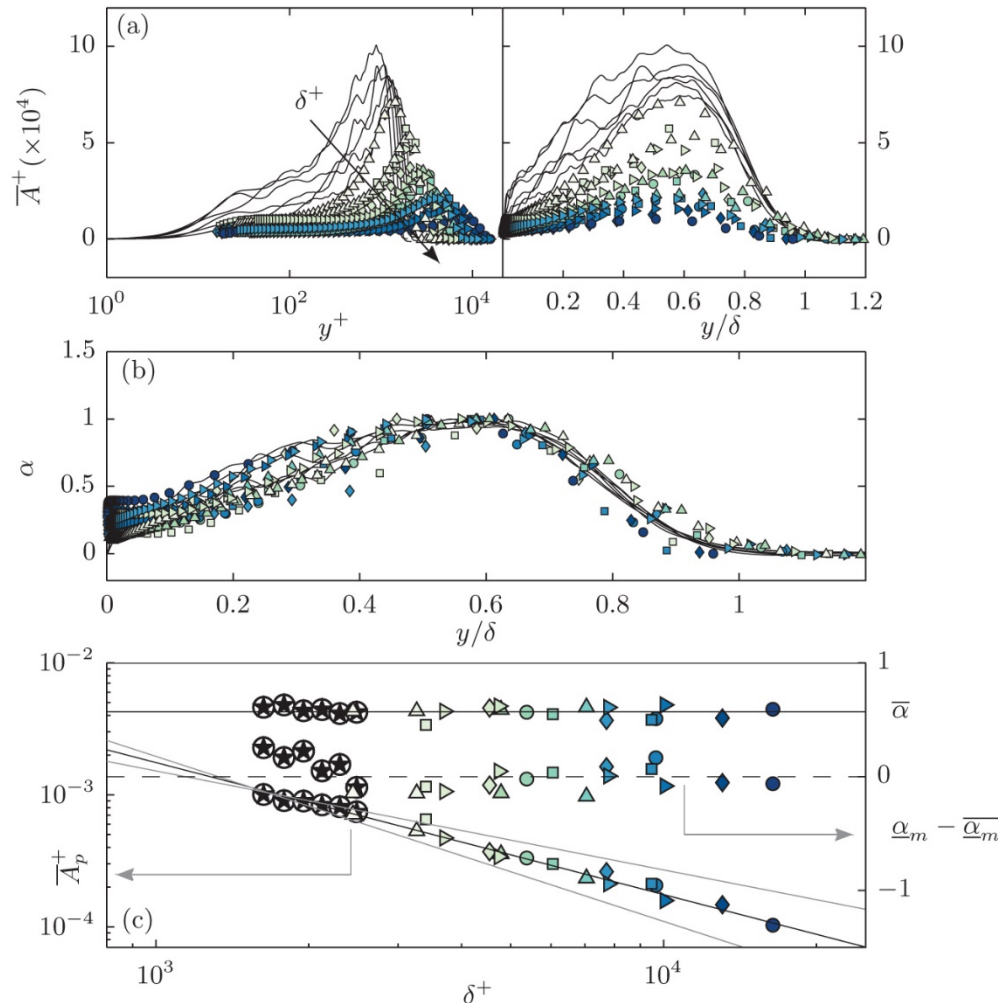
(Morrill-Winter et al. EiT 2015)

symbol	$\delta^+$	$U_\infty$ (m/s)	$u_\tau$ (m/s)	$\nu/u_\tau$ ( $\times 10^{-6}$ m)	$l^+$	Facility
$\triangle$	2400	10.1	0.37	43	11.5	HRNBLWT
$\triangle$	3300	10.1	0.36	45	11.1	HRNBLWT
$\square$	3400	4.4	0.16	95	5.3	FPF
$\triangleright$	3700	15.2	0.54	30	16.9	HRNBLWT
$\diamond$	4500	6.6	0.23	67	7.5	FPF
$\triangleright$	4700	15.1	0.52	31	16.3	HRNBLWT
$\triangle$	4800	10.0	0.34	47	10.7	HRNBLWT
$\circ$	5400	8.8	0.30	52	9.6	FPF
$\blacksquare$	6100	4.2	0.14	100	5.0	FPF
$\triangle$	7000	10.0	0.33	48	10.5	HRNBLWT
$\diamond$	7700	6.6	0.22	68	7.3	FPF
$\triangleright$	7800	15.3	0.51	31	16.3	HRNBLWT
$\blacksquare$	9500	4.3	0.14	108	4.7	FPF
$\bullet$	9700	8.8	0.29	53	9.4	FPF
$\triangleright$	10100	15.3	0.50	32	15.6	HRNBLWT
$\diamond$	13100	6.6	0.21	71	7.1	FPF
$\bullet$	16400	8.8	0.28	55	9.1	FPF

Table 1. Experimental parameters.  $U_\infty$  is the free stream velocity and  $l$  is the representative length of the sensor.

# Behaviour of Mean Inertia Term

(Morrill-Winter et al. Eif 2015)



$$\bar{A} = \alpha(x, y) \bar{A}_p(x)$$

$$\bar{\alpha} := \delta^{-1} \int_0^\infty \alpha(x, y) dy,$$

$$\underline{\alpha}(x, y) := \alpha(x, y) / \bar{\alpha}$$

# Representation of Mean Inertia Term

The above findings yield

$$\frac{d^2U^+}{dy^{+2}} + \frac{dT^+}{dy^+} + \underbrace{\bar{\alpha}(\delta^+) \bar{A}_p^+(\delta^+)}_{1/\delta^+} \underline{\alpha}(x^+, y^+) = 0$$

(empirically found to equal  $1.003/\delta^+$ )

Where it is now noted that it can be analytically shown (via integration) that the bracketed product is identically equal to  $1/\delta^+$ . Thus,

$$\frac{d^2U^+}{dy^{+2}} + \frac{dT^+}{dy^+} + \frac{1}{\delta^+} \underline{\alpha}(y^+, \delta^+) = 0$$

The desired  $1/\delta^+$  dependence has been extracted, but  $\underline{\alpha}$  still equals  $\underline{\alpha}(y^+, \delta^+)$ .

# Transforming the Inertia Terms

The aim now is to remove the  $y^+$  dependence of  $\underline{\alpha}$  on the inertial domain (layer IV). This is done by simultaneously transforming both the TI and MI (A) terms.

$$\tilde{T} := T^+ + \frac{1}{\delta^+} \int_0^{y^+} \Lambda(s, \delta^+) ds,$$

where,  $\Lambda(y^+, \delta^+) := \underline{\alpha}(y^+, \delta^+) - \underline{\alpha}_m(\delta^+)$ , and  $\underline{\alpha}_m(\delta^+) := \underline{\alpha}(y_m, \delta^+)$ . Using these definitions, (3.2) becomes

$$\frac{d^2 U^+}{dy^{+2}} + \frac{d\tilde{T}}{dy^+} + \frac{\alpha_m}{\delta^+} = 0.$$

While  $\underline{\alpha}_m = \underline{\alpha}_m(\delta^+)$  is a possibility, data covering over a decade in  $\delta^+$  fortuitously indicate that  $\underline{\alpha}_m(\delta^+) = \text{const.} \approx 0.46$ .

Thus, we recover a form of the mean equation that is like that for channel flow on the inertial domain.

# Transformed Inertia Term Profiles

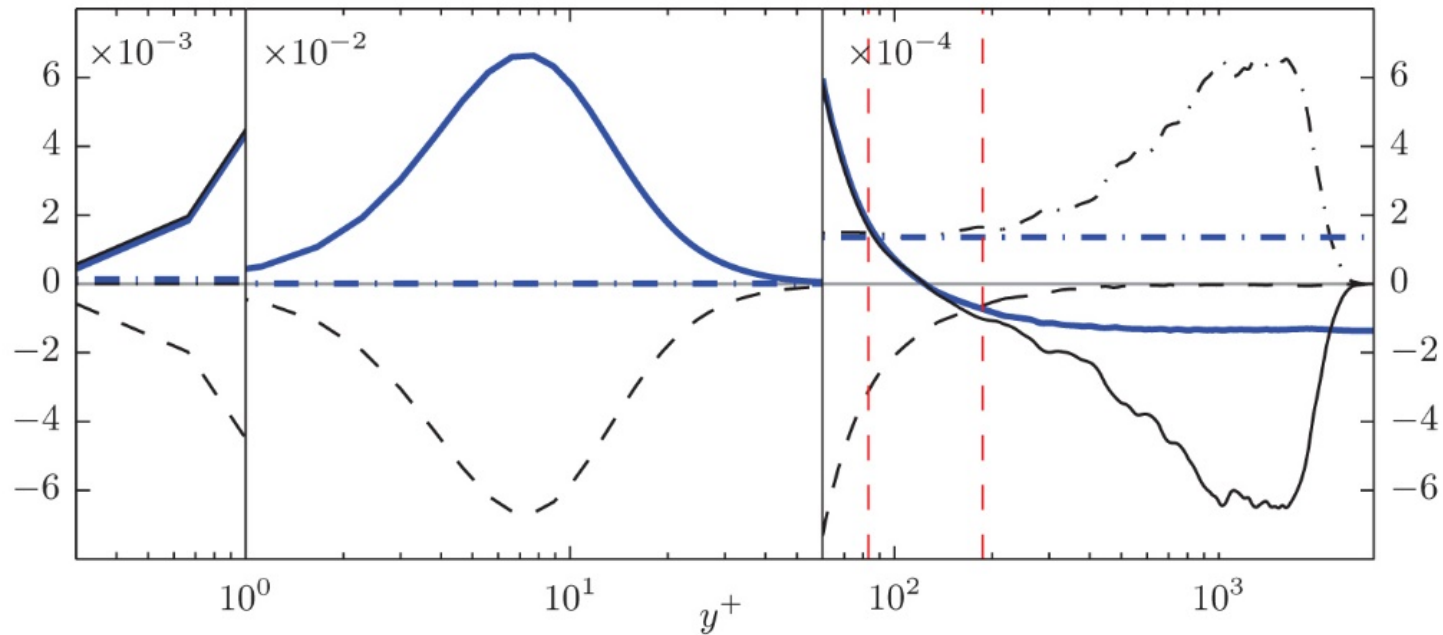


FIGURE 3. The inner-normalized terms present in (1.1) - thin (black) lines and (3.5) - thick (blue) lines at  $\delta^+ \simeq 2,400$  employing the DNS of Sillero *et al.* (2013). The  $VF^+$  is denoted by dashed lines (---), whereas  $TI^+$  and  $\bar{A}^+$  is given by (—) and (---), respectively. The transformed Reynolds stress gradient ( $d\tilde{T}/dy^+$ ) and  $\underline{\alpha}_m(\delta^+)/\delta^+$  in (3.5) are denoted by (---) and (—), respectively. The gray line simply marks zero. The vertical dashed (red) lines are limits of the intermediate region provided by (4.4). Note that this is a continuous plot; however, we have employed different multipliers in different wall-normal regions so as to re-scale the distributions for visual clarity.

# Layer III Properties

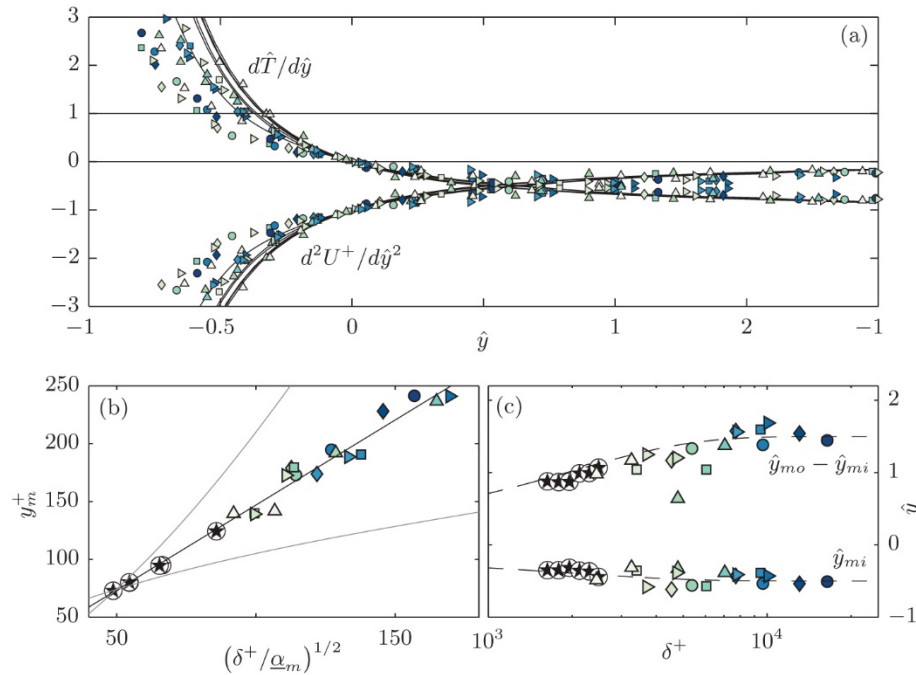
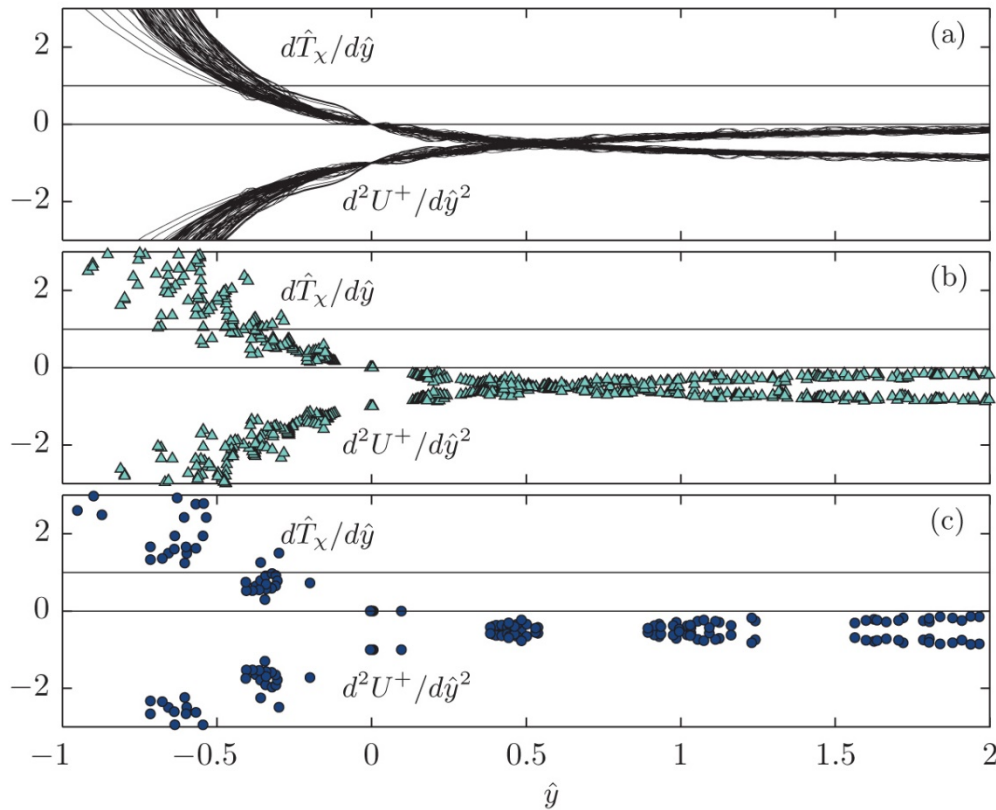


FIGURE 4. Scaling in the intermediate regime. (a) The terms of (4.2) on along  $\hat{y}$  for different  $\delta^+$ . The (—) and  $\otimes$  are the DNS of Sillero *et al.* (2013) and the symbols are given in table 1. (b) The wall position of the zero-crossing in the transformed Reynolds stress gradient (or peak in the Reynolds stress) versus the  $(\delta^+/\alpha_m)^{1/2}$ . The solid black line is  $y_m^+ = 1.47(\delta^+/\alpha_m)^{1/2}$ . The gray lines are  $y_m^+ = 10.5(\delta^+/\alpha_m)^{1/4}$  and  $y_m^+ = 0.21(\delta^+/\alpha_m)^{3/4}$ , which are added to give perspective to the intermediate scaling. The intercepts were chosen such that all the fits would pass through the lowest  $\delta^+$  point. (c) The nominal width ( $\hat{y}_{mo} - \hat{y}_{mi}$ ) and the beginning ( $\hat{y}_{mi}$ ) of the scaling domain. The (---) lines are best fit lines of the form  $\hat{s} = \hat{s}_1 + (\hat{s}_0 - \hat{s}_1)e^{\delta^+/\Delta_c}$ . Where  $\hat{s}$  is any hat variable,  $\hat{s}_0$  and  $\hat{s}_1$  are the starting and ending values of  $\hat{s}$ , respectively, and  $\Delta_c$  is a constant.

# Invariant Layer Hierarchy



Note that  $\chi$ , rather than  $\beta$ , now denotes the hierarchy parameter.

FIGURE 6. The terms present in (5.6) at multiple values of  $\chi$  at three different  $\delta^+$ . (a)  $\delta^+ = 2400$ , (b)  $\delta^+ = 7000$  and (c)  $\delta^+ = 16400$ . The DNS is given by (—) and  $\otimes$ , where the experimental symbols can be found in table 1.

# Conclusions

- For channel flow one can:
  - 1) **Begin with the mean equation**
  - 2) **Transform it to an invariant form, and**
  - 3) **Analytically integrate it to yield an asymptotically universal log law similarity solution**
- For the ZPG boundary layer a scenario is given indicating that one can:
  - 1) **Begin with the mean equation**
  - 2) **Transform the MI and TI terms to look like channel flow**
  - 3) **Transform this equation to an invariant form, and**
  - 4) **Analytically integrate it to yield an asymptotically universal log law similarity solution**
- This scenario recovers the empirical observation that the asymptotic slope of the logarithmic mean velocity profile is the same in boundary layers, pipes and channels.
- Structure predicted is consistent with Townsend's attached eddy notions, the self-similar hierarchy of the McKeon and Sharma (2010) resolvent model, and the physical structure of uniform momentum zones and vortical fissure revealed by Meinhart and Adrian (1995).